Free Vibrations of Cylindrical Shells Partially Suspended on Elastic Foundations

Haryadi Gunawan Tj*, Takashi Mikami**, Shunji Kanie***, Motohiro Sato****

* Graduate Student, Graduate School of Eng., Hokkaido University, Kita 13 Nishi 8, Kita-ku, Sapporo 060-8628
** Dr. of Eng., Professor, Dept. of Civil Eng., Hokkaido University, Kita 13 Nishi 8, Kita-ku, Sapporo 060-8628
*** Dr. of Eng., Assoc. Prof., Dept. of Civil Eng., Hokkaido University, Kita 13 Nishi 8, Kita-ku, Sapporo 060-8628
**** Dr. of Eng., Instructor, Dept. of Civil Eng., Hokkaido University, Kita 13 Nishi 8, Kita-ku, Sapporo 060-8628

Free vibration characteristics of cylindrical shells partially buried and suspended on elastic foundations are presented by means of the hybrid finite element method. Shell governing equations based shape functions in the longitudinal direction are used instead of the usual simple polynomials. The non-uniformities of the foundations in the circumferential and longitudinal directions are handled by a Fourier series and an element mesh strategy, respectively. Effects of the foundation arrangements, length of the gap, and foundation parameters on the natural frequencies of the vibrating systems are investigated. Results for both symmetric and asymmetric vibrations are presented systematically.

Key Words: Cylindrical Shells, Elastic Foundations, Finite Element Method

1. Introduction

In practical applications, cylindrical shells are found in the form of tanks, water ducts, pipes, and many others. These shells are widely used because of their strength characteristics. Therefore, investigation of the dynamical behavior of the shells becomes a great importance in the design of such structures. The present paper deals with the free vibrations of cylindrical shells partially suspended on elastic foundations. The shell is placed over a gap so that only parts of it are resting on the foundations.

Lakis *et al.*[1,2] has developed the hybrid finite element formulation of cylindrical shells based on the analytical shape functions which are derived from the shell governing equations. Yang[3] has investigated the whole buried pipelines in the elastic foundations subjected to sinusoidal seismic loads by using the finite element method. Free vibrations of the whole buried cylindrical shells in Winkler and Pasternak foundations have been studied thoroughly by Palliwal *et al.*[4,5] using the direct solution to the governing equations of motion. However, cylindrical shells are generally laid on or placed in the elastic foundation so that the foundation only covers certain parts of the shell in the circumferential direction. Free vibrations of cylindrical shells simply supported at both ends with a non-uniform elastic foundation in the circumferential direction have been investigated by Amabili *et al.*[6] based on the Rayleigh-Ritz method. By using the method, formulations need to be modified extensively if other boundary conditions are prescribed at the ends of the shells. Moreover, the elastic foundations have to be assumed uniformly distributed over the whole cylinder length in the longitudinal direction. Gunawan *et al.*[7] has studied the static and free vibration characteristics of cylindrical shells partially buried in the elastic foundations based on the finite element method where the usual simple polynomials have been used as shape functions in the longitudinal direction. However, excessive number of elements has been used in order to have converged solutions.

In general, the foundation is not uniform due to ground contour irregularities. For an extreme case, the shell may be suspended across a gap. Reference related to the problem of cylindrical shells partially suspended on the elastic foundations is not available. Therefore, this paper presents the dynamic characteristics of the problem undergoing the linear free vibration by using the hybrid finite element method. In the analysis, the discretization is conducted by dividing the shells into ring shaped elements so that the present method can be directly applied for shells with a non-uniform distribution of the foundations either in the longitudinal or in the circumferential direction. The effects of foundation parameters and length of the gap on the natural frequencies are

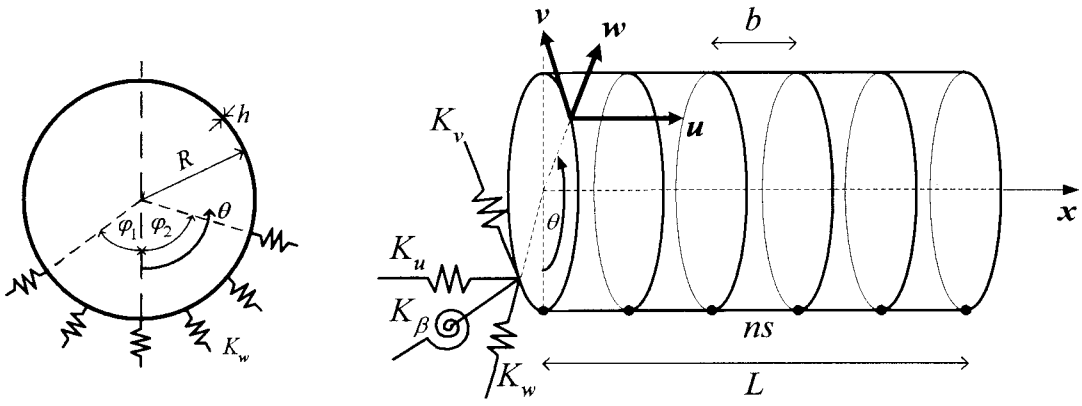

(a) Geometry (b) Generalized model

Fig.1. Geometry and generalized model

systematically presented for both symmetric and asymmetric vibrations. Many numerical results for different arrangements of the foundations are given in this paper.

2. Analytical Model and Formulation

The structure is an isotropic thin elastic cylindrical shell with Young's modulus E, Poisson's ratio υ, radius of the middle surface R, thickness h, and length L. The foundation is represented by continuous elastic (axial, circumferential, radial, and rotational) springs on a limited arc. In the analysis, the spring coefficients are assumed to be constant along the enclosed arc. The axial, circumferential, radial, and rotational spring coefficients are K_u, K_v, K_w, and K_β, respectively. φ_1 and φ_2 are the angles that define the enclosed arc. The geometry of the structure and the generalized model with reference directions are shown in Fig.1.

The displacement of a point on the middle surface in the axial, circumferential, and radial directions are indicated by u, v, and w, respectively. The rotation angle β is defined as the first derivative of w with respect to x. The displacement functions which include the symmetric (superscript S) and asymmetric (superscript U) deformations with respect to the $\theta = 0$ are given by:

$$\begin{aligned}
u(x,\theta) &= \sum_{m=0}^{M}\left[U_m^{S}(x)\cos(m\theta)+U_m^{U}(x)\sin(m\theta)\right]\\
v(x,\theta) &= \sum_{m=0}^{M}\left[V_m^{S}(x)\sin(m\theta)+V_m^{U}(x)\cos(m\theta)\right]\\
w(x,\theta) &= \sum_{m=0}^{M}\left[W_m^{S}(x)\cos(m\theta)+W_m^{U}(x)\sin(m\theta)\right]\\
\beta(x,\theta) &= \sum_{m=0}^{M}\left[B_m^{S}(x)\cos(m\theta)+B_m^{U}(x)\sin(m\theta)\right]
\end{aligned} \tag{1}$$

where M is total number of circumferential waves used to truncate the series.

For the sake of brevity, the formulation is explained only for a symmetric system. Formulation for the asymmetric system can be derived analogously as that of the symmetric one. The longitudinal shape functions are assumed to be in the form of:

$$\begin{aligned}
U_m^{S}(x) &= A_m^{S}\, e^{\mu_m x/R}\\
V_m^{S}(x) &= B_m^{S}\, e^{\mu_m x/R}\\
W_m^{S}(x) &= C_m^{S}\, e^{\mu_m x/R}
\end{aligned} \tag{2}$$

where A_m^S, B_m^S, and C_m^S are constants for a typical circumferential wave, m. μ_m is the characteristic value which can be found by substituting Eq.(2) into the following Sanders equations of thin cylindrical shells:

$$\mathcal{L}_1(u,v,w)=0;\ \mathcal{L}_2(u,v,w)=0;\ \mathcal{L}_3(u,v,w)=0 \tag{3}$$

where $\mathcal{L}_1$, $\mathcal{L}_2$, and $\mathcal{L}_3$ are the differential operators of the shell equations (without the foundation) in the axial, circumferential, and radial directions. Details of the operators may be found in the papers by Lakis *et al.*[1,2]. On the substitution of Eq.(2) into Eq.(3), three simultaneous linear equations in A_m^S, B_m^S, and C_m^S can be obtained. For a non-trivial solution, determinant of the coefficient matrix has to be zero. After simplifications, for $m \neq 0$, the eighth order characteristic polynomial can be obtained and given below:

$$\sum_{i=0}^{8} a_{mi}\mu_m^i = 0 \tag{4}$$

where a_{mi} is the coefficients of the polynomial. Solution of Eq.(4) leads to eight complex characteristic roots (μ_{mj}, where j = 1, 2, 3 ... 8). As the constants A_m^S, B_m^S, and C_m^S are not independent, the complete longitudinal shape functions can be rewritten as follows:

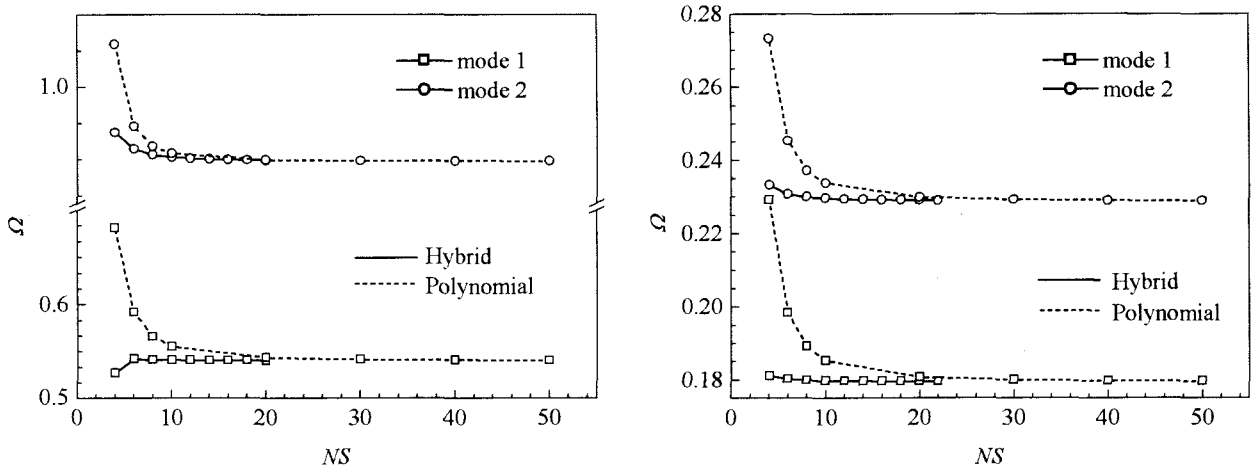

(a) $R/L = 0.05$, $R/h = 20$ (b) $R/L = 0.20$, $R/h = 200$

Fig.2. Convergence of Ω (Symmetric vibration, *SS*, $\upsilon = 0.30$, $K_w L/E = 0.003$, $\varphi_1 = \varphi_2 = \varphi = \pi/3$, and $M = 20$)

$$U_m^S(x) = \sum_{j=1}^{8} \alpha_{mj}^S \, C_{mj}^S \, e^{\mu_m x/R}$$
$$V_m^S(x) = \sum_{j=1}^{8} \gamma_{mj}^S \, C_{mj}^S \, e^{\mu_m x/R} \qquad (5)$$
$$W_m^S(x) = \sum_{j=1}^{8} C_{mj}^S \, e^{\mu_m x/R}$$

where α_{mj}^S and γ_{mj}^S are constants. It is worthwhile to mention that the asymmetric system leads to the identical characteristic polynomial as for the symmetric system (Eq.(4)) so that $\mu_{mj}^S = \mu_{mj}^U = \mu_{mj}$, $\alpha_{mj}^S = \alpha_{mj}^U$, but $\gamma_{mj}^S = -\gamma_{mj}^U$. For $m = 0$, the system is separated into torsional and non-torsional systems. Details on the formulation can be found in the paper by Lakis *et al.*[2] and therefore is not explained here.

Finite element discretization is done in usual way to derive the stiffness and mass matrices of a shell element:

$$\mathbf{K}_S = \int_A \mathbf{B}^T \mathbf{D} \mathbf{B} \, dA; \quad \mathbf{M}_S = \rho \int_V \mathbf{N}^T \mathbf{N} \, dV \qquad (6)$$

and the stiffness matrix of the foundation:

$$\mathbf{K}_F = \int_A \mathbf{N}^T \mathbf{k}_f \, \mathbf{N} \, dA \qquad (7)$$

where $\mathbf{B}$, $\mathbf{D}$, $\mathbf{N}$, $\mathbf{k}_f$, and ρ are the matrix which links the strains to the displacements, an elasticity matrix, the total shape function matrix, a diagonal matrix containing the foundation distribution functions, and mass per unit volume of the shell, respectively. Full explanations on this matter can be found in the paper by Gunawan *et al.*[7].

In the analysis, the non-uniform distribution of the foundation in the longitudinal direction is discretized by the element mesh strategy as in the finite element method. Finally, the global equation can be written as

$$\mathbb{K} \, \mathbf{d} = \omega^2 \mathbb{M} \, \mathbf{d} \qquad (8)$$

where $\mathbb{K}$, $\mathbb{M}$, $\mathbf{d}$, and ω are the global stiffness matrix, the global mass matrix, the total nodal displacement vector, and natural frequency of the vibrating system, respectively. For convenience, the non-dimensional frequency parameter $\Omega = \omega L \sqrt{\rho(1-\upsilon^2)/E}$ is used through out this paper.

3. Convergence Studies

Although it is not shown here, convergence of the results depends on the total number of elements (*NS*) and the total number of circumferential waves (*M*). In term of convergence, *NS* is more significant for shells with small values of *R/L* and *R/h*, while *M* is more significant for shells with large values of *R/L* and *R/h*. Based on the investigation, $M = 20$ gives good accuracy to the results. Numerical calculations were carried out to investigate the convergence behavior of the solution as a function of the total number of elements, *NS*. For comparisons, the results obtained by using the simple polynomials[7] as the longitudinal shape functions are also presented. The computations used the following parameters: $\upsilon = 0.30$, $K_w L/E = 0.003$, and $\varphi_1 = \varphi_2 = \varphi = \pi/3$. The shell is assumed to be simply supported at both ends and the foundation is considered to be uniformly distributed over the whole cylinder length.

Convergence behaviors of two different geometries of shells are presented in Fig.2. From the figure, it can be concluded that the hybrid formulation gives a better convergence behavior. In addition, the shape functions based on the shell governing equations are still applicable for the problem under consideration. However, the behavior of convergence for first mode obtained by the hybrid method for relatively small and

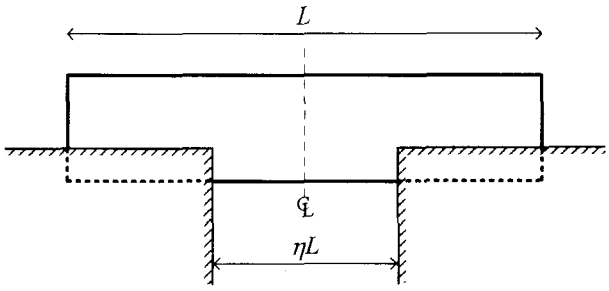

Fig.3. Case 1.

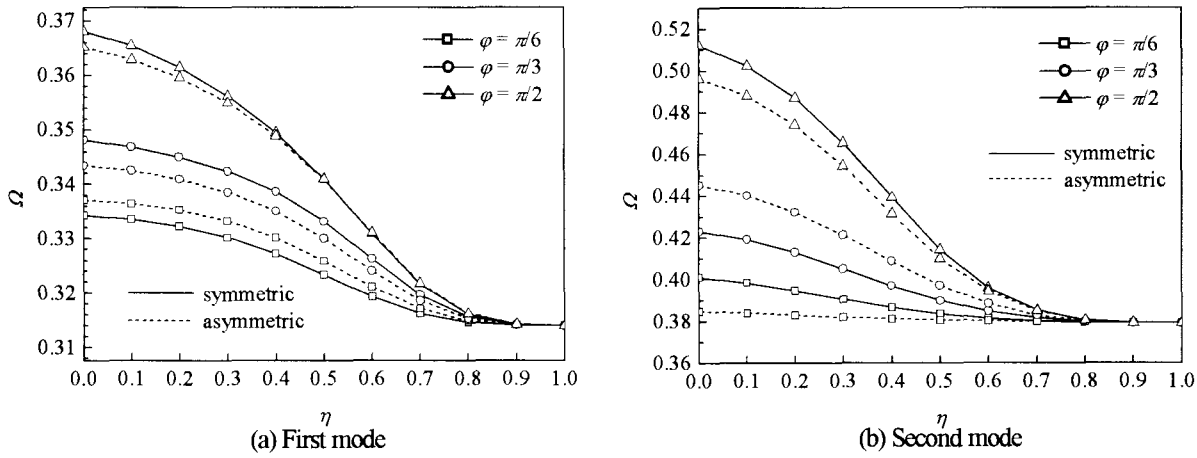

(a) First mode (b) Second mode

Fig.4. Variations in Ω with η for different values of φ. (CC, $R/L = 0.20$, $R/h = 100$, and $K_w L/E = 0.002$)

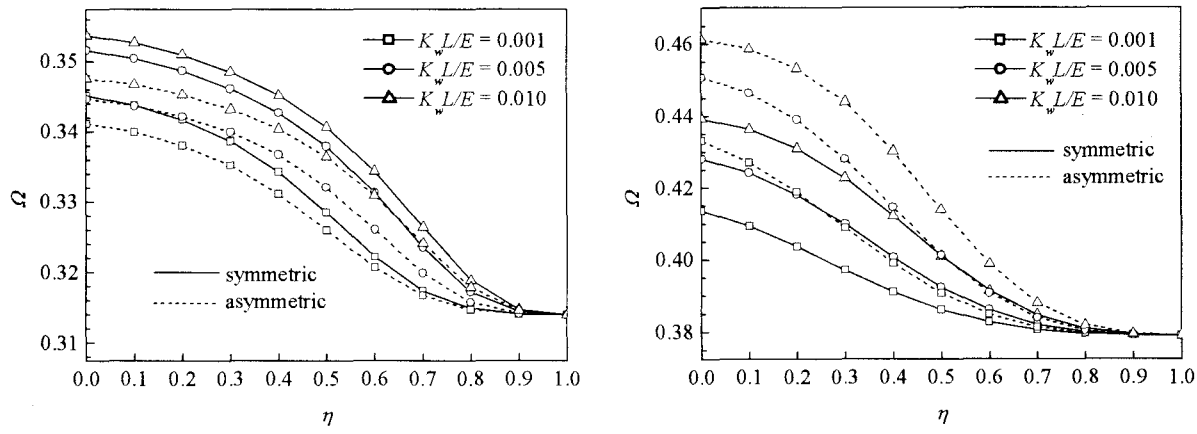

(a) First mode (b) Second mode

Fig.5. Variations in Ω with η for different values of $K_w L/E$. (CC, $R/L = 0.20$, $R/h = 100$, and $\varphi = \pi/3$)

thick shell (Fig.2.(a)) at $NS = 4$ is different from the other modes. It exhibits a numerical error due to large values of $\mu_m x$ for the given shell parameters.

The next example compares the results with those obtained by Amabili *et al.*[6]. The shell considered had the following properties: $\upsilon = 0.30$, $E = 206$ GPa, $\rho = 7800$ Kg/m^3, $R = 300$ mm, $L = 1000$ mm, $h = 3$ mm, $K_w = 1.18\times10^{10}$ N/m^3 and $\varphi = \pi/2$. Natural frequencies for the first four modes are 230.5(227.8) Hz, 231.2(230) Hz, 327.8(326) Hz, and 366.3(360.2) Hz. The values in parenthesis correspond to the results obtained by Amabili *et al.*[6]. The results are in good agreement.

4. Numerical Results

In this section, cylindrical shells partially suspended on the elastic foundations were analyzed. Four different cases which correspond to different arrangements of the foundations are

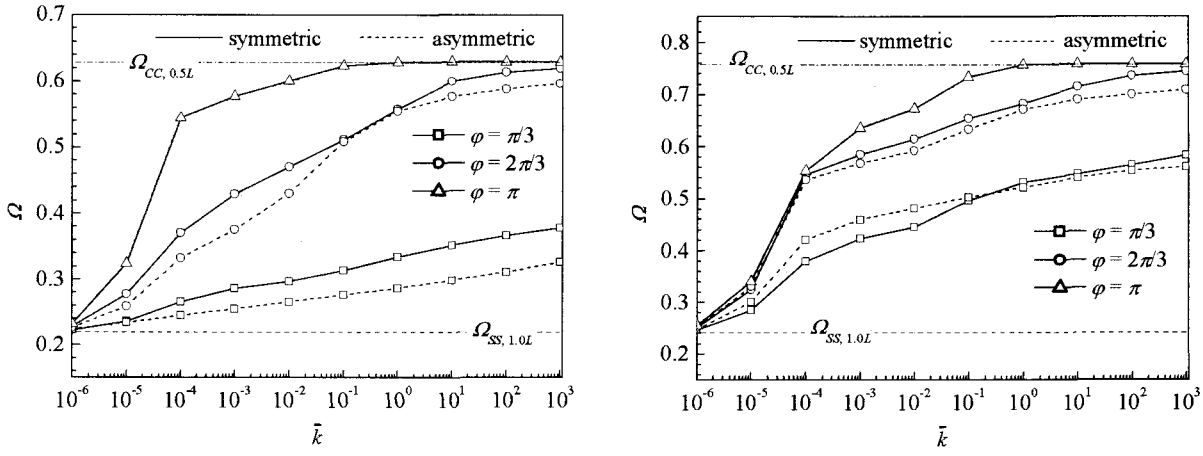

(a) First mode (b) Second mode

Fig.6. Variations in Ω with $\bar{k}$ for different values of φ. (*SS*, $R/L = 0.10$, $R/h = 100$, and $\eta = 0.5$)

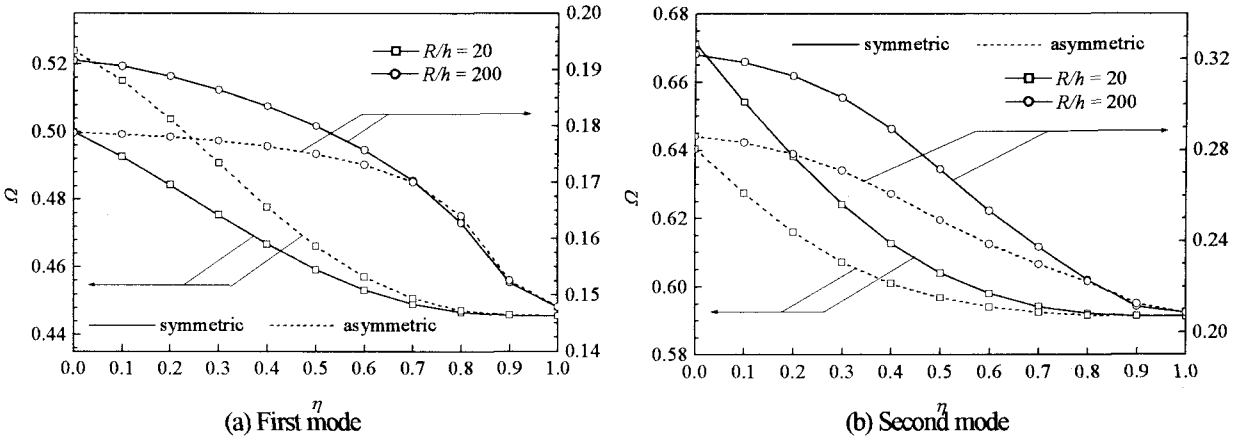

(a) First mode (b) Second mode

Fig.7. Variations in Ω with η for different values of R/h. (*SS*, $R/L = 0.10$, $K_w L/E = 0.002$, and $\varphi = \pi/3$)

presented. The variations in the natural frequencies with the length of the gap and with the foundation parameters are given in order to asses the dynamical characteristics of the shells under consideration. In all figures and tables, the length of the gap is represented by ηL where η is the gap parameter. $\eta = 0$ corresponds to the case of the shell resting on the elastic foundation and $\eta = 1$ represents the shell in the air. Two types of boundary conditions are considered, namely *SS* and *CC* which correspond to simply supported and clamped at both ends, respectively. Unless otherwise stated, the computations used the following parameters: $\upsilon = 0.30$, $K_u = K_v = K_\beta = 0$, $K_w \neq 0$, $\varphi_1 = \varphi_2 = \varphi$, $NS = 20$, and $M = 20$.

4.1. Case 1

Fig.3 shows the shell partially suspended on the elastic foundations. The gap is located at the middle.

For the first computation, a shell with *CC*, $R/L = 0{,}20$ and $R/h = 100$ is analyzed. Fig.4 shows the variations in Ω with η for different values of φ. As η increases, Ω gradually decreases. Both symmetric and asymmetric vibrations show a similar behavior. Fig.5 shows the variations in Ω with η for different values of $K_w L/E$.

The second computation was carried out for shell with *SS*, $R/L = 0.10$, $R/h = 100$, and $\eta = 0.5$. Fig.6 shows the variations in Ω with $\bar{k}$ ($= K_u L/E = K_v L/E = K_w L/E = K_\beta/(EL)$) for different values of φ. The axial, circumferential, radial, and rotational springs are included in order to provide an appropriate boundary condition for a clamped edge. The figure presents the effects of the foundation parameters and gives a validation to the present results at the same time. It is clear from the figure that as $\bar{k}$ increases, Ω increases. For a particular case when $\varphi = \pi$ and extremely large values of $\bar{k}$, Ω coincides with $\Omega_{CC,\,0.5L}$, the natural frequency parameter of shell (without foundation) clamped at both ends with $0.5L$ in length. In other words, clamped boundary conditions are simulated by applying extremely stiff springs.

Fig.7 shows the effects of thickness on the variations in Ω for the shell with given parameters. In the figure, the left and right hand side scales correspond to the results for $R/h = 20$ and $R/h = 200$, respectively as shown by the arrows. It can be seen that the decrement rates are different from each other. The

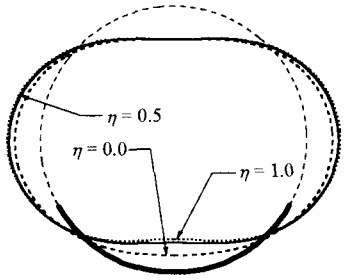

First symmetric mode

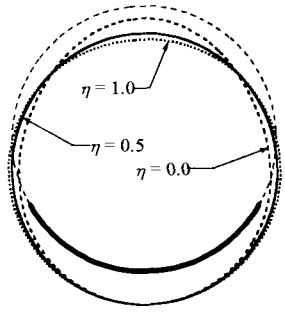

Second symmetric mode

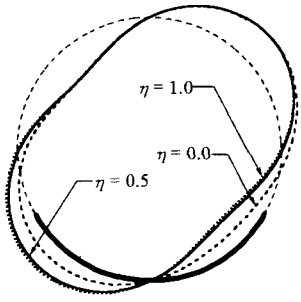

First asymmetric mode

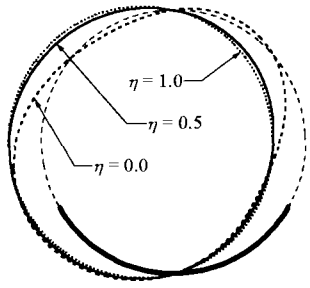

Second asymmetric mode

Fig.8. Radial mode shapes. (*SS*, $R/L = 0.10$, $R/h = 20$, $K_w L/E = 0.002$, and $\varphi = \pi/3$)

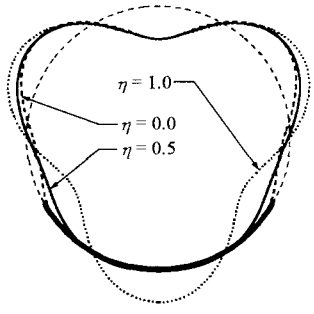

First symmetric mode

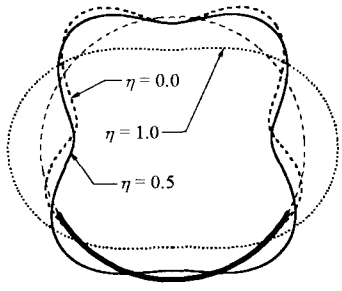

Second symmetric mode

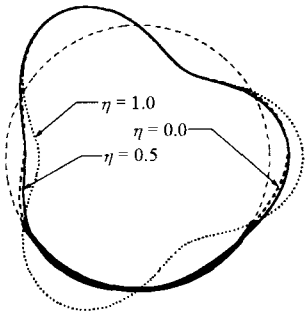

First asymmetric mode

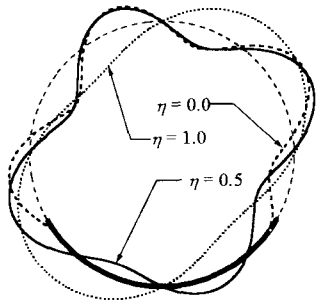

Second asymmetric mode

Fig.9. Radial mode shapes. (*SS*, $R/L = 0.10$, $R/h = 200$, $K_w L/E = 0.002$, and $\varphi = \pi/3$)

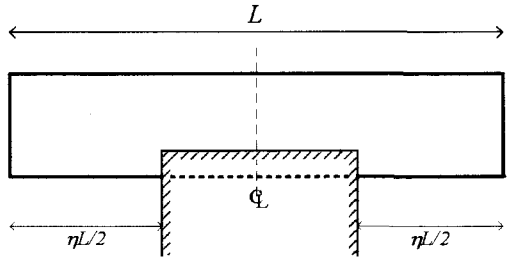

Fig.10. Case 2.

Table 1. First mode.
($R/L = 0.10$, $R/h = 50$, and $K_w L/E = 0.002$)

η	φ	Ω_η/Ω_1			
		SS		CC	
		symmetric	asymmetric	symmetric	asymmetric
0.0	$\pi/6$	1.353	1.185	1.064	1.030
	$\pi/3$	1.402	1.468	1.130	1.095
	$\pi/2$	1.598	1.658	1.171	1.282
0.2	$\pi/6$	1.352	1.184	1.064	1.030
	$\pi/3$	1.401	1.466	1.130	1.095
	$\pi/2$	1.596	1.656	1.170	1.282
0.4	$\pi/6$	1.343	1.177	1.063	1.030
	$\pi/3$	1.390	1.455	1.127	1.093
	$\pi/2$	1.580	1.642	1.167	1.276
0.6	$\pi/6$	1.315	1.156	1.061	1.028
	$\pi/3$	1.356	1.421	1.115	1.087
	$\pi/2$	1.531	1.598	1.151	1.250
0.8	$\pi/6$	1.242	1.110	1.053	1.024
	$\pi/3$	1.272	1.338	1.085	1.071
	$\pi/2$	1.419	1.476	1.114	1.182
1.0	–	$\Omega_1 = 0.259$		$\Omega_1 = 0.447$	

Table 2. Second mode.
($R/L = 0.10$, $R/h = 50$, and $K_w L/E = 0.002$)

η	φ	Ω_η/Ω_1			
		SS		CC	
		symmetric	asymmetric	symmetric	asymmetric
0.0	$\pi/6$	1.158	1.205	1.320	1.220
	$\pi/3$	1.348	1.254	1.395	1.541
	$\pi/2$	1.562	1.485	1.710	1.603
0.2	$\pi/6$	1.158	1.204	1.320	1.220
	$\pi/3$	1.346	1.253	1.394	1.540
	$\pi/2$	1.558	1.482	1.708	1.603
0.4	$\pi/6$	1.152	1.193	1.311	1.213
	$\pi/3$	1.329	1.249	1.385	1.528
	$\pi/2$	1.527	1.460	1.686	1.589
0.6	$\pi/6$	1.135	1.158	1.270	1.184
	$\pi/3$	1.274	1.233	1.339	1.465
	$\pi/2$	1.446	1.388	1.605	1.516
0.8	$\pi/6$	1.093	1.095	1.169	1.115
	$\pi/3$	1.173	1.181	1.222	1.304
	$\pi/2$	1.315	1.253	1.404	1.334
1.0	–	$\Omega_1 = 0.454$		$\Omega_1 = 0.492$	

Note: Ω_η corresponds to the value of Ω for a shell with gap parameter η

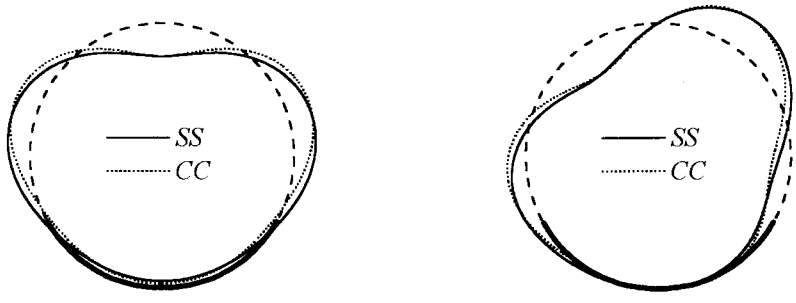

(a) Symmetric (b) Asymmetric

Fig.11. Radial mode shapes. (First mode, *SS*, $R/L = 0.10$, $R/h = 50$, $K_w L/E = 0.002$, $\varphi = \pi/3$, and $\eta = 0.6$)

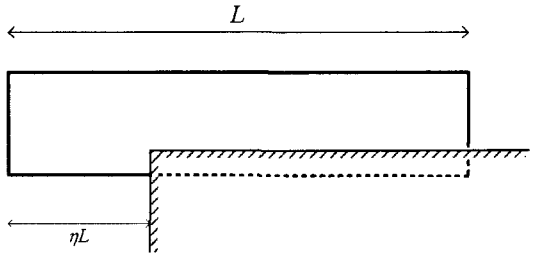

Fig. 12. Case 3.

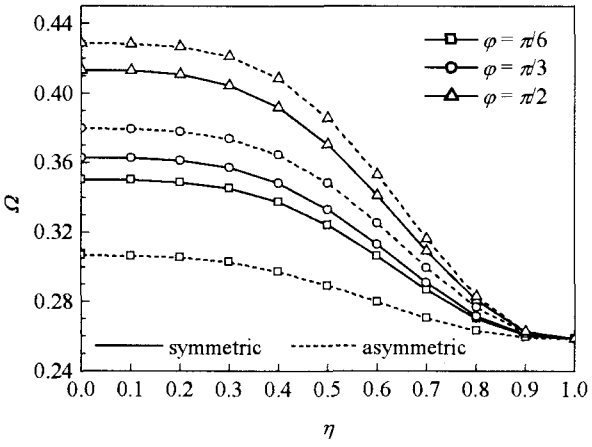

Fig.13. Variations in Ω with η for different values of φ. (First mode, *SS*, $R/L = 0.10$, $R/h = 50$, and $K_w L/E = 0.002$)

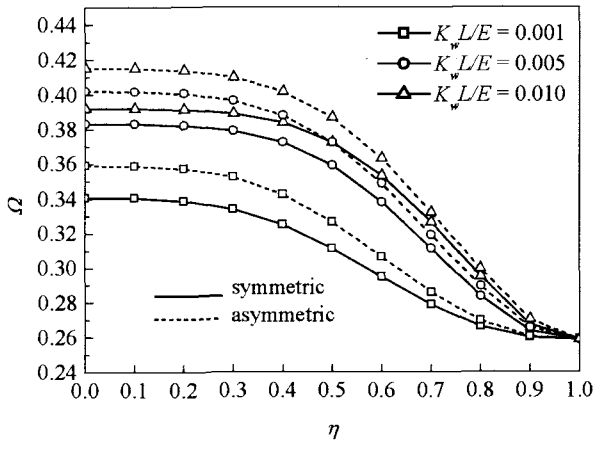

Fig.14. Variations in Ω with η for different values of $K_w L/E$. (First mode, *SS*, $R/L = 0.10$, $R/h = 50$, and $\varphi = \pi/3$)

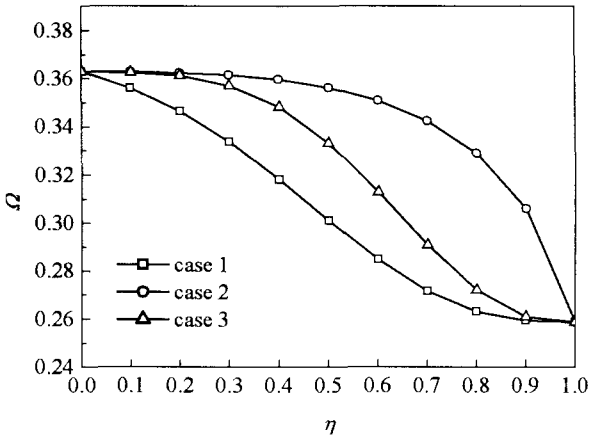

(a) Symmetric

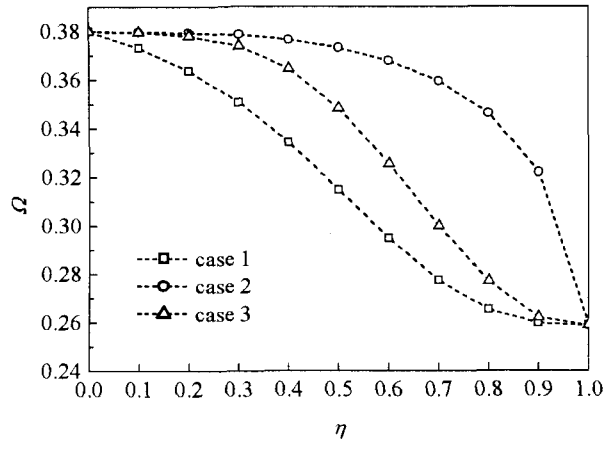

(b) Asymmetric

Fig.15. Variations in Ω for different cases. (First mode, *SS*, $R/L = 0.10$, $R/h = 50$, $K_w L/E = 0.002$, and $\varphi = \pi/3$)

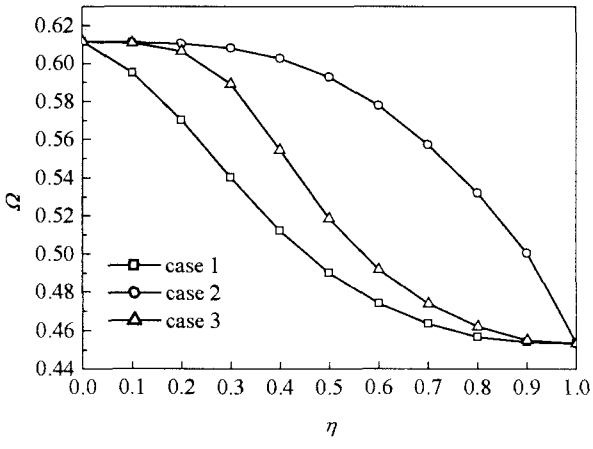

(a) Symmetric

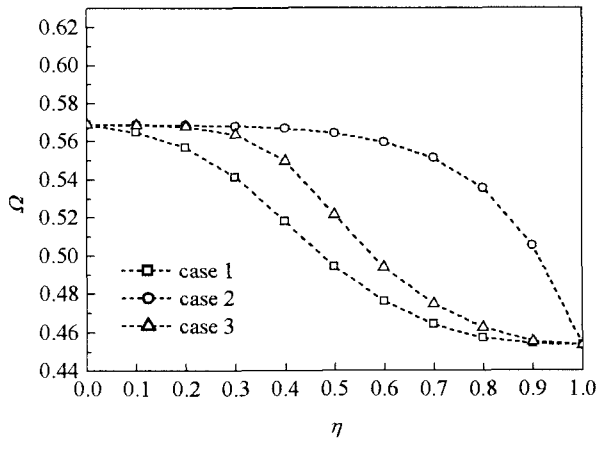

(b) Asymmetric

Fig.16. Variations in Ω for different cases. (Second mode, *SS*, $R/L = 0.10$, $R/h = 50$, $K_w L/E = 0.002$, and $\varphi = \pi/3$)

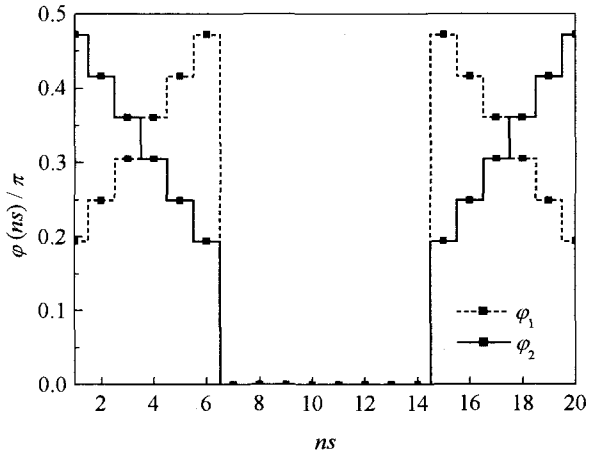

Fig. 17. Distribution of the enclosed angles.

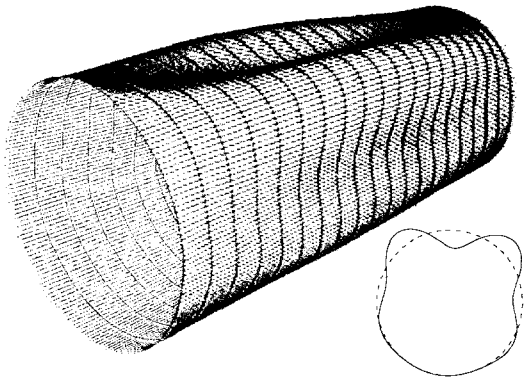

(a) First mode, $\Omega = 0.1760$

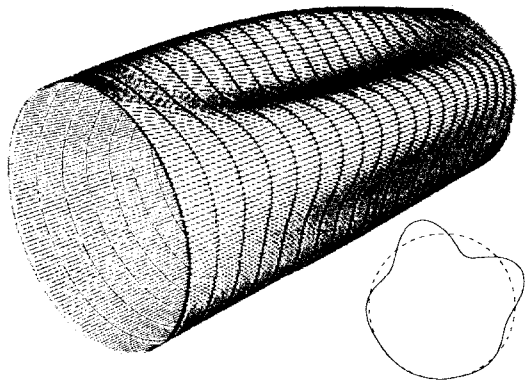

(b) Second mode, $\Omega = 0.1783$

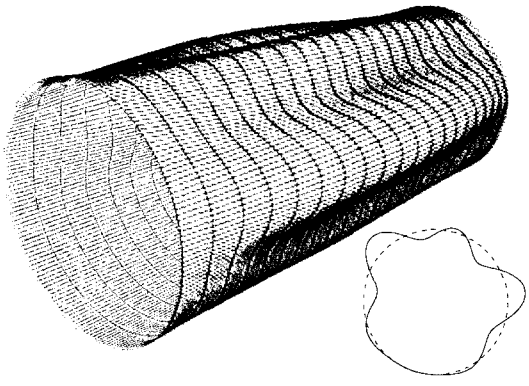

(c) Third mode, $\Omega = 0.2331$

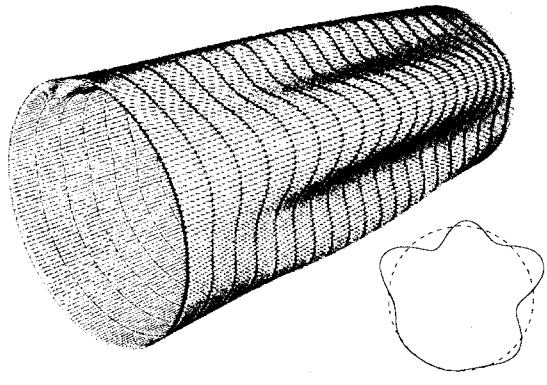

(d) Fourth mode, $\Omega = 0.2378$

Fig.18. Overall radial mode shapes. (*SS*, $R/L = 0.20$, $R/h = 200$, $K_w L/E = 0.003$, and $\eta = 0.4$)

decrement rates at small values of η for shells with small values of R/h were found to be greater than those of shell with large value of R/h. Fig.8 and Fig.9 show the variations in radial mode shapes of shells with given parameters for various values of η. In the figures, the thickest line represents the enclosed arc.

4.2. Case 2

The second case is represented by Fig. 10, where the $K_wL/E = 0.002$. Ω_η / Ω_1 of *SS* and *CC* with various values of η and φ are presented in Table 1 and Table 2 for the first and second modes, respectively. In contrast with the results for *SS*, the values of Ω_η / Ω_1 of *CC* for second mode are larger than those for first mode. Fig.11 shows the radial mode shapes of shells with the given parameters.

4.3. Case 3

In this section, the shell shown in Fig.12 is assumed to be simply supported at both ends with the following parameters: $R/L = 0.10$ and $R/h = 50$. The results of Ω for different values of φ and K_wL/E are plotted against the gap parameter η in Fig.13 and Fig.14, respectively. Similar distributions can be observed as those in the previous cases. Fig.15 and Fig.16 show the variations in Ω with η for different cases. From the figures, it can be concluded that case 1 is the most sensitive.

4.4. Case 4

In this section, a numerical example of shell partially suspended on non-uniform elastic foundations in the longitudinal direction is presented. The shell is assumed to be simply supported at both ends with the following parameters: $R/L = 0.20$, $R/h = 200$, $K_wL/E = 0.003$, and $\eta = 0.4$. The distribution of enclosed angles in the longitudinal direction is given in Fig.17. The values of φ_1 and φ_2 at ns–th element were discretized to have a constant value across the element. Fig.18 shows the overall radial mode shape of the problem.

foundation is located at the middle of the shell. In this section, these following parameters are used: $R/L = 0.10$, $R/h = 50$, and

5. Conclusions

Present semi-analytical finite element method has been shown to be useful for analyzing cylindrical shells partially suspended on the elastic foundations. The hybrid formulation based on shell governing equations without existence of the foundation is still applicable for the problem considered. Convergence behavior shows a better improvement rather than that of the usual simple polynomials based shape functions. In the present method, arbitrary distribution of the foundations in the circumferential direction may be handled by a Fourier series while the distribution in the longitudinal direction can be modeled by an element mesh strategy.

Many numerical results associated with the different arrangements of the foundations have been presented. The effects of the foundation parameters such as the spring stiffness and the enclosed angle on the vibration characteristics of the problem have been studied. The applicability of present method for general cases of shells on non-uniform elastic foundations has been shown. From this study, it can be concluded that the present formulation is suitable for the problem considered due to its generality, simplicity, and further development possibilities. Further studies will address the interactive behavior of the shell, foundations, and liquid inside the shell.

References

1) Lakis, A.A. and Paidoussis, M.P., Dynamic Analysis of Axially Non-Uniform Thin cylindrical Shells., J. Mech. Eng. Sci., 14(1), pp.49-71, 1972.
2) Lakis, A.A. and Sinno, M., Free Vibration of Axisymmetric and Beam-Like Cylindrical Shells, Partially Filled With Liquid., Int. J. for Numerical Methods in Eng., 33, pp.235-268, 1992.
3) Yang, R., Kameda, H. and Takada, S., Shell Model FEM Analysis of Buried Pipelines under Seismic Loading., Bull. Disas. Prev. Res. Inst., Kyoto University, 38(3), pp.115-146, 1988.
4) Paliwal, D.N., Pandey, R.K. and Nath, T., Free Vibrations of Circular Cylindrical Shell on Winkler and Pasternak Foundation., Int. J. Pressure Vessels and Piping, 69(1), pp.79-89, 1996.
5) Paliwal, D.N., Kanagasabapathy, H. and Gupta, K.M., The Large Deflection of an orthotropic Cylindrical Shell on a Pasternak Foundation, Comp. and Struc., 31(1), pp.31-37, 1995.
6) Amabili, M. and Dalpiaz G., Free Vibration of Cylindrical Shells with Non-Axisymmetric Mass Distribution on Elastic Bed., Meccanica, 32, pp.71-84, 1997.
7) Gunawan, H., Sato, M., Kanie, S. and Mikami, T., Static and Free Vibration Analysis of Cylindrical Shells on Elastic Foundation., JSCE J. Struc. Eng., 50A, pp.25-33, 2004.

(Received September 17, 2004)